



On the potential of solid state LED strips utilizing an organic color converter for non-line of sight visible light communication

AMANUEL ASSEFA, PO-JUI CHEN, XUAN LONG HO, AND JONATHON DAVID WHITE*

Department of Photonics Engineering, Yuan Ze University, Zhong-Li District, Taoyuan City, Taiwan
*whitejd@xiaotu.ca

Abstract: LED strip lighting can provide high quality uniform shadow-free diffuse lighting at low cost as numerous emission sources are controlled by a single transformer. Organic LEDs offer the additional advantages of UV free emission and, for visible light communication, picosecond fluorescent lifetimes allowing the whole visible spectrum to be used without filters. Using parameters determined experimentally for solid-state LED strip lighting and fluorescent lifetimes typical of organic phosphors as the input for a Monte Carlo based ray-tracing simulation, we evaluate the potential bandwidths obtainable for indoor communication. Our work suggests that raw data transfer rates of 4 to 10 Mbps are obtainable in a standard 5m by 5m by 3m room compatible with Internet of Things (IoT) applications.

© 2017 Optical Society of America

OCIS codes: (060.0060) Fiber optics and optical communications, (060.2605) Free-space optical communication.

References and links

1. Ericsson, "Ericsson Mobility Report on the Pulse of the Networked Society," (Nov 2015), p.10 (<http://www.ericsson.com/res/docs/2015/mobility-report/ericsson-mobility-report-nov-2015.pdf>).
2. S. Zvanovec, P. Chvojka, P. Haigh, and Z. Ghassemloooy, "Visible Light Communications towards 5G," *Radioengineering* **24**(1), 1–9 (2015).
3. K. Lee, H. Park, and J. Barry, "Indoor Channel Characteristics for Visible Light Communications," *IEEE Commun. Lett.* **15**(2), 217–219 (2011).
4. A. Azhar, T. Tran, and D. O'Brien, "A Gigabit/s Indoor Wireless Transmission Using MIMO-OFDM Visible-Light Communications," *IEEE Commun. Lett.* **25**(2), 171–174 (2013).
5. H. Li, X. Chen, J. Guo, and H. Chen, "A 550 Mbit/s real-time visible light communication system based on phosphorescent white light LED for practical high-speed low-complexity application," *Opt. Express* **22**(22), 27203–27213 (2014).
6. T. Komine and M. Nakagawa, "Fundamental analysis for visible-light communication system using LED lights," *IEEE Trans. Consum. Electron.* **50**(1), 100–107 (2004).
7. H. Q. Nguyen, J. Choi, M. Kang, Z. Ghassemloooy, D. Kim, S. Lim, T. Kang, and C. G. Lee, "A MATLAB-based simulation program for indoor visible light communication system," *Communication Systems Networks and Digital Signal Processing (CSNDSP)*, 2010 7th International Symposium on, Newcastle upon Tyne, 537–541 (2010).
8. S. Rajagopal, R. D. Roberts, and S. K. Lim, "IEEE 802.15.7 visible light communication: modulation schemes and dimming support," *IEEE Commun. Mag.* **50**(3), 72–82 (2012).
9. X. Huang, S. Chen, Z. Wang, J. Shi, Y. Wang, J. Xiao, and N. Chi, "2.0-Gb/s Visible Light Link Based on Adaptive Bit Allocation OFDM of a Single Phosphorescent White LED," *IEEE Photonics J.* **7**(5), 1–8 (2015).
10. M. Esmail and H. Fathallah, "Indoor visible light communication without line of sight: investigation and performance analysis," *Photonic Netw. Commun.* **30**(2), 159–166 (2015).
11. C. Chen, D. Basnayaka and H. Haas, "Non-line-of-sight Channel Impulse Response Characterisation in Visible Light Communications," presented at IEEE ICC 2016 – Optical Networks and Systems (22–26 May, 2016).
12. J. Y. Sung, C. W. Chow, and C. H. Yeh, "Is blue optical filter necessary in high speed phosphor-based white light LED visible light communications?" *Opt. Express* **22**(17), 20646–20651 (2014).
13. M. Sajjad, P. Manousiadis, H. Chun, D. Vithanage, S. Rajbhandari, A. Kanibolotsky, G. Faulkner, D. O'Brien, P. Skabara, I. Samuel, and G. Turnbull, "Novel Fast Color-Converter for Visible Light Communication Using a Blend of Conjugated Polymers," *ACS Photonics* **2**(2), 194–199 (2015).
14. [S. Hejduk, K. Witas, J. Latal, J. Vitasek, J. Bocheza, and V. Vasinek, "Simple and Universal Current Modulator Circuit for Indoor Mobile Free-Space-Optical Communications Testing," *AEEE* **12**(1), 1–9 (2014).
15. Y. Liu, C. Yeh, and C. Chow, "Alternating-Signal-Biased System Design and Demonstration for Visible Light Communication," *IEEE Photonics J.* **5**(4), 7901806 (2013).

16. National Optical Astronomy Observatory, "Recommended Light Levels," p. 4 (https://www.noao.edu/education/QLTkit/ACTIVITY_Documents/Safety/LightLevels_outdoor+indoor.pdf).
17. Lighting Research Center (Rensselaer Polytechnic Institute), "Reflectance," p. 1 (<http://www.lrc.rpi.edu/education/learning/terminology/reflectance.asp>).

1. Introduction

Network data demand is increasing between 60% and 100% year-on-year with 75% of his bandwidth being used indoors. The adoption of Internet of Things (expected to reach 28.1 billion devices by 2021 [1]) will only increase the demand for bandwidth. It is difficult to imagine how existing radio frequency (RF) communication technology will be able to meet this need due to restrictions on licensed wavelength and interference problems. In addition, radio frequencies are also not suitable for use in sensitive environments such as hospitals, aircraft and mines due to interference with sensitive electronics and where security is of utmost importance.

Clearly, in any VLC application, lighting must be the first priority while VLC capabilities are value added. Up to date the vast majority of research into VLC has concentrated on configurations using a central source with a few high powered or an array of pcLED (phosphor coated LED)'s mounted downwards from ceilings [3–6]. Komine's [6] group performed some of the first numerical simulations of data rate in this predominately line-of-sight (LOS) configuration while later work by Lee's group [7] incorporated reflections off walls into the model. C. G. Lee [3] further incorporated wall and ceiling characteristics into the model. Experimentally, transmission at 1 Gb/s has been demonstrated using multiple input multiple output (MIMO) links [4], while X Chen [5] achieved 550 Mb/s with significantly less complexity. A key focus in most of this (experimental) work has been the development of modulation schemes that offer high bandwidth without affecting lighting [8-9].

While these centralized pcLEDs are good for VLC, the high intensity generated from a very small source results in eye discomfort, less visual acuity and increased glare making them less than ideal from a lighting perspective. In contrast, diffuse lighting creates a much more visually pleasing light distribution without glare or shadowing. Diffuse lighting can be achieved by many ways. For example, using diffusive covers for the light source can control the degree of dispersion to a certain extent. A better option is to use indirect lighting in which the sources are hid from the eye and only reach the observer after multiple reflections. Recently the group of M Esmail [10] have predicted the performance of non-line-of-sight (NLOS) for a number of configuration scenarios while Harold Haas's [11] group have analyzed the channel input response function in such configurations.

Diffuse lighting can also be obtained by employing LED strip (also called tape or ribbon) lights which have many advantages over independent high power LEDs. Firstly, since LED strip lights can use one centralized AC to DC converter and a DC bus line to distribute the load to multiple strips in parallel, the conversion of AC to DC is both efficient and cost effective. Secondly, numerous light sources on the strip allow for shadow-free diffuse, uniform ambient lighting. Thirdly, installation of LED strips is easy. While pcLED based strip lighting offers superior performance from a lighting perspective than a centralized source, they are not optimum from a VLC perspective as they suffer the same limitations as pcLEDs – the long PL lifetime of the phosphor.

It is generally accepted that for pcLEDs, in order to achieve high speed transmission, it is necessary to use a blue filter at the receiver end to mitigate the long PL lifetime of the phosphor (See [12] for a counter opinion). Other than the added cost of the filter, the use of a filter sharply reduces the intensity at the detector. An alternative to this is to employ materials that have short PL lifetimes, i.e., organic semiconducting polymers. These materials have a very short PL lifetime (< 1 ns), high radiative rates, high photoluminescence quantum yields and can be employed either in completely organic devices [2] or to replace the phosphor as a color converter on a GaN LED. In the latter configuration, Samuel et al. [13], using BBEHP-PPV and MEH-PPV having fluorescence lifetimes of 825ps and 380ps respectively, have

obtained modulation bandwidths (electrical-electrical) of 200MHz (~40 times higher than commercially available pcLEDs) in direct line-of-sight applications.

An ideal solution, from a lighting and VLC perspective would be strip lighting in a NLOS system making use of an organic color converter. In this work, we present a preliminary investigation into the capabilities of such a system based on the optical constants of the organic color converter of Ref. 13. Monte Carlo based ray-tracing is used to investigate the flux distribution (for lighting) and NLOS impulse response and rms delay times (for communication) for a room lighted by LED strips with an organic color converter. In the investigated configuration, a single current modulator provides input to all LED strips in a room [14] that could work in conjunction with AC power line modulation [15].

The paper is laid out as follows. In section 2 the room design, methodology, and simulation parameters are introduced. In section 3, we present the results of the study in terms of flux, impulse response and rms delay for a few room configurations. Finally in section 4, we present a short discussion of these results and state conclusions.

2. Room design, parameters, and methodology

Figure 1 presents a schematic of the model room and Table 1 presents the corresponding parameters used in the Monte Carlo Ray Tracing simulation. In the NLOS configuration investigated here, the LED strips are placed on a platform with the emission normal in the vertical direction to ensure that there is no direct light path from the source to the detector and that the illumination source is not visible to the room occupants. Multiple light pathways eliminate shadowing. A single modulated power supply is located in the center of the room on the ceiling to provide modulated power to LED strips. This location minimizes the propagation delay of the signal and ensures that each LED strip receives the signal at the same time.

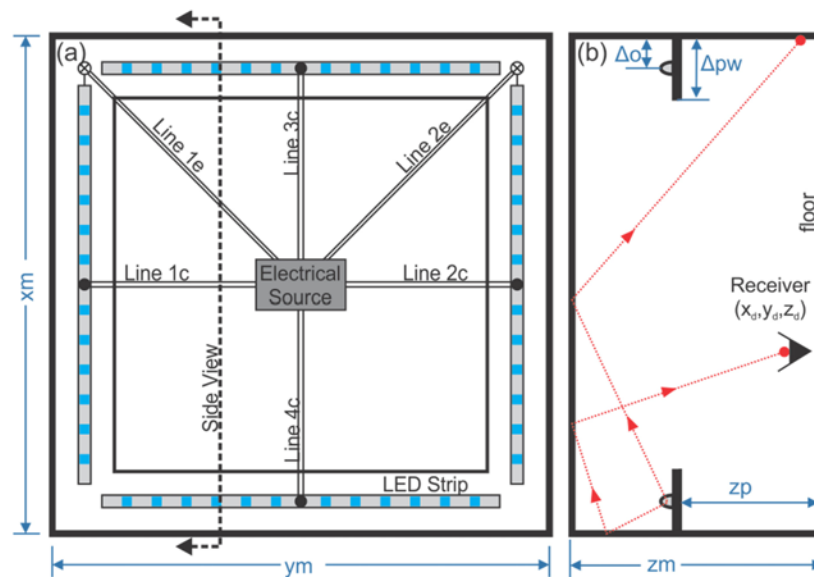


Figure 1. Schematic of room layout (a) Top view (b) Side view. LED strips (located on a platform near the roof) are shown in gray with LEDs indicated in blue. Dotted red lines represent sample photon trajectories. Double lines supply power to the LED strips from the central transformer. (Simulations and experiments are carried out for different connected lines.)

Electrical lines take the signal to one or more LED strips (modeled using the emission parameters of an off-the-shelf LED strip, Table 1). In each LED strip, individual LED units (3

LED in series) are placed in parallel every 1.6 cm. The signal propagates down the strip with a propagation delay (velocity factor) of ~40% of the speed of light. As a result the time at which an LED receives the signal is directly correlated with its distance from the source. This is included in the model as the electric delay of a photon. Electricity (signal) is input from either the end or center of each 5m LED strip.

Table 1. Simulation Parameters

	Parameter	Symbol	Value
Room	Room Depth, Width, Height	x_m, y_m, z_m	500 cm, 500 cm, 300 cm
	Platform Width, Height	$z_p, \Delta p_w$	260 cm, 15 cm
	Reflectivity (Wall, Ceiling, Floor)	$R_{wall}, R_{ceiling}, R_{floor}$	0.85, 0.85, 0.12 (Lambertian, $n = 2$)
	Electrical Source Location	(x_s, y_s, z_s)	(250, 250, 300) cm
LED strip	Type: 5050 SMD, 2700K	n_{LED}	60 LEDs/m, 5m long`
	Offset from wall	Δo	7.5 cm
	Emission normal	n	Vertical (up)
	Total Length of Strips	L	5, 10 or 20 meters
	Luminous Power	P_{LED}	21.6 lumen/LED
	Semi-angle at half power	$\phi_{1/2}$	30°
	Luminous Intensity	I_v	$I_v(\phi) = I_v(0)\cos^5(\phi)$
	Inorganic Phosphor lifetime	τ_{phos}	500 ns
	Electric signal velocity	$v_{electric}$	$0.4c = 1.2 * 10^{10}$ cm/s
Simulation	Organic color converter lifetime	τ_{org}	0.4 and 0.85 ns [Ref. 13]
	Photons/LED	N_{LED}	20,000,000
Detector/Receiver	Detector Location	(x_d, y_d, z_d)	$(0 < x_d < x_m, 0 < y_d < y_m, z = 0)$ cm
	Detector Field of View	FOV_{det}	80°
	Detector Area	A_{det}	1 cm ²
	Detector Efficiency	$\eta_{detector}$	12%

The measured angular dependence of the luminous intensity (I_v) of each LED was well fit by a Lambertian radiation pattern [6]:

$$I_v(\phi) = I_v(0) \cos^m(\phi) \quad (1)$$

where:

$$m = -\ln(2) / \ln(\cos(\phi_{1/2})) \quad (2)$$

and $\phi_{1/2}$ is the semi-angle at half illuminance of the LED. While $m = 4$ ($\phi_{1/2} = 33^\circ$) was the best experimental fit to the distribution, except as noted, for the simulation we use $m = 5$ ($\phi_{1/2} = 30^\circ$) to allow comparison with published work. Scattering (reflection) coefficients from the white walls, ceiling and dark floor were measured and found to be Lambertian ($n = 2$). The values were within the range specified in Ref [17].

Monte Carlo based ray-tracing (home written in Java) was used to trace the trajectories of twenty million photons from each of the 60 to 240 LEDs (depending on the lighting configuration) through multiple reflections from the ceiling, walls and floor until absorption or detection. For those photons arriving at the detector the total transit time (electrical + optical time of flight) and the number of reflections were recorded.

From the above data the total irradiance (Lux), impulse response function and the root mean square of the delay spread (τ_{RMS}) were calculated by summing up all the photons reaching the detector. Irradiance (I) on the detector in Lux was calculated as follows:

$$I(x_d, y_d, z_d) = \frac{N_d}{N} \times \frac{(n_{LED} \times L \times P_{LED})}{A_{det}} [Lux] \quad (3)$$

where N_d is the number of photons reaching the detector, N is the total number of simulated photons, A_{det} is the area of the detector and the quantity in brackets is the total emitted power in Lumen.

The total transit time of the i^{th} photon (t_i) was calculated by adding its optical transit time to the electrical delay. Based on the average time of arrival for all photons reaching the detector ($\langle \tau \rangle$), the root mean square delay spread at each point in the room was calculated:

$$\tau_{RMS}(x, y, z) = \sqrt{\frac{\sum_{i=1}^N (t_i - \tau)^2}{N_d}} \quad (4)$$

In calculating the maximum data transfer rate (bps), the simplest form of modulation-Intensity modulation direct detection utilizing On-off key (OOK)–was assumed. That is,

$$R_b = \min\left(\frac{1}{10\tau_{rms}}\right) [bps] \quad (5)$$

3. Results

Before applying the simulation to the 5m by 5m by 3m room, a basement utility room was used to test the simulation predictions. The commercial 5050 LED strip was placed on a platform ($z_p = 260\text{cm}$, $\Delta p_w = 15\text{cm}$, $\Delta o = 7.5\text{cm}$) along the longest wall of the 4 m x 2.56 m x 2.85 m high room and the strip excited from the end of the room (only Line 1e in Fig. 1 connected). Excellent agreement was obtained between the predicted illuminance and that recorded using the ThorLabs PM100 optical detector. As the maximum bandwidth was limited to the kHz range by the long-lived inorganic phosphor, the following discussion will focus on the simulation of strips incorporating the organic color converter.

3.1 Illuminance distribution

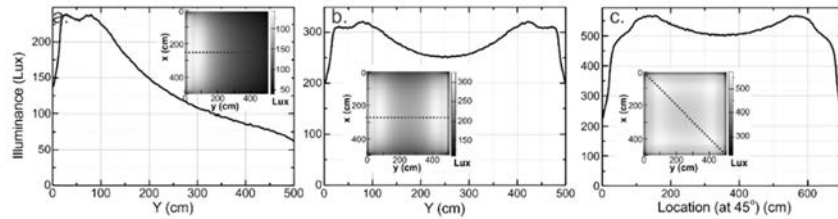


Fig. 2. Illuminance at floor level for (a) one sided, (b) two sided, and (c) four sided illumination. The main figure shows a cross-section of the illuminance taken at the dashed line in the gray scale insets.

As the primary purpose for any lighting system is lighting, we first present the illuminance for three lighting configurations in Fig. 2 for the 5m by 5m by 3m high room. The distribution in Fig. 2(a) represents illumination from only one side of the room (Line 1 (either e or c) in Fig. 1(a) connected) with a single 5m LED strip. Although this configuration allowed for fairly uniform illumination ($\pm 10\%$) for the utility room, it is clearly not a feasible solution for the wider room. In addition the light levels, except on the left side of the room, is below that recommended by NOAO [16] of 250 Lux. The distribution in Fig. 2(b) is the case of two-sided illumination (Line 1 and Line 2 in Fig. 1(a) connected) with two 5m LED strips. Lighting across the room is much more evenly distributed with the lighting level in the majority of the room exceeding 250 Lux. In Fig. 2(c) the case of four sided illumination

(Lines 1, 2, 3, 4 in Fig. 1(a) connected) utilizing four 5m LED strips is presented. Illumination is quite uniform (except close to the walls) and is near the recommended lighting value of 500 Lux for normal office work [16].

Table 2. Comparison of the illuminance and rms delay spread for different lighting configurations

Lighting	Configuration Signal Input	Illuminance (Lux)				RMS delay spread (ns)		
		Mean	Center	Min*	Max	Mean	Min	Max*
1 sided	From end	127	125	46 (-64%)	243 (+91%)	24.5	16.6	28.8
	From center					24.3	17.6	28.3
2 sided	From end	254	252	109 (-57%)	325 (+28%)	24.7	20.1	27.8
	From center					24.5	21.1	26.6
4 sided	From center	508	504	467 (-8%)	574 (+13%)	24.5	22.5	22.3

Table 2 summarizes mean Lux and the variation in lighting level for the three lighting configurations. The minimum Lux is taken 25cm from the wall. Both one-sided and two-sided configurations result unacceptable variations across the room with variations of the already low lighting level of over $\pm 50\%$. Excluding the corners of the room, the absolute lighting level (in Lux) and the approximately $\pm 10\%$ variation in illuminance (when corners excluded) for 4-sided illumination make this the preferred choice.

3.2 Root mean square (RMS) delay

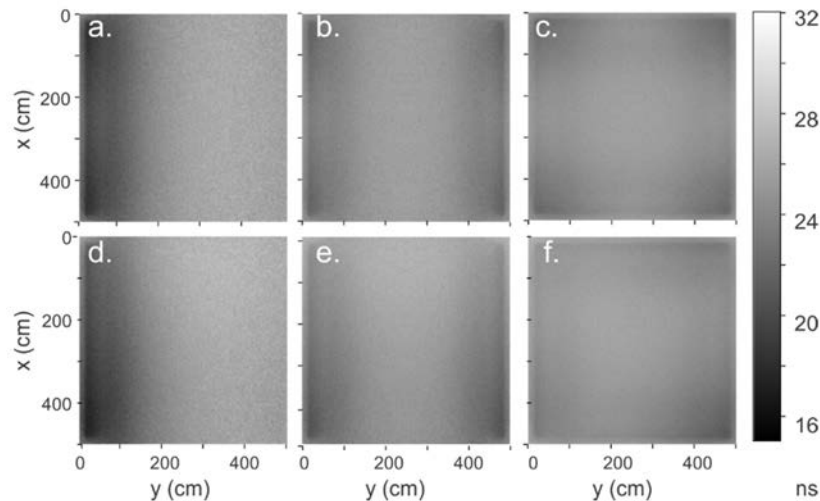


Fig. 3. Distribution across the room of the rms delay spread for (left) one sided, (middle) two sided, and (right) four sided illumination. In the top (bottom) images, the electrical signal is input at the strip end (center).

Once the requirements for lighting have been met one can optimize for VLC. Figure 3 presents the rms delay spread curves for the three lighting configurations with different electrical lines turned on. In Fig. 3(a) where only electrical Line 1e (in Fig. 1) is connected, the minimum τ_{RMS} is below the end farthest from the electrical input. This is not unexpected as (1) the optical path length (for 1 reflection) is shorter for locations nearest the LED strip, and (2) while photons from the LED's closest to electrical input are emitted earlier in time, they have a longer optical path length to follow in order to reach the detector. Conversely, the rms delay spread is greatest on the side of the room opposite the electrical input of the LED strip. This again is not unexpected as (1) the optical path length (for 1 reflection) is longer for locations nearest the LED strip, and (2) photons from the LED's closest to electrical input are emitted earlier in time, and have a shorter optical path length to follow in order to reach the

detector. In Fig. 3(d) where only electrical Line 1c connected (signal input to the center of the LED strip), the minimum rms delay spread remains under the LED strip farthest away from the signal input while the maximum rms delay spread occurs far away from the strip.

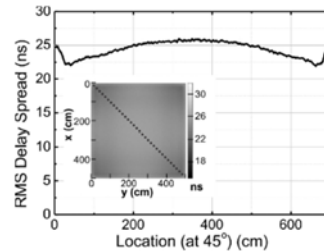


Fig. 4. RMS delay spread for four sided illumination with the signal input from center of room. (inset) rms delay spread across the room. Dashed line indicates location of cross-section.

For two sided excitation (Fig. 3(b), lines 1e and 2e connected and Fig. 3(e), lines 1c and 2c connected), there is a dramatic increase in the minimum rms delay spread due to the much greater average optical path length at these points. This is accompanied by a slight decrease in the more important maximum rms delay spread. Finally, with four sided excitation from the center (Fig. 3(f), lines 1c, 2c, 3c, and 4c in Fig. 1(a) connected), the rms delay spread is similar at all points in the room with the maximum occurring the middle of the room. The cross-section of the rms delay spread shown in Fig. 4 shows this more clearly. The maximum rms delay spread is seen to be ~ 25 ns in the center of the room and at edges with a slight dip ~ 50 cm from the wall to 22.5 ns. These results are summarized in Table 2. As seen in the table, in moving from single to symmetric four sided illumination the spread in the rms delay spread is reduced from 12 ns to 3 ns and the limiting maximum rms delay has been reduced by 3.5 ns from 28.8 to 25.3 ns. Making use of Eq. (5), the maximum raw data rate (R_b) obtainable with organic coated strip LEDs is ~ 4 Mbps without equalization for this room.

3.3 Impulse response

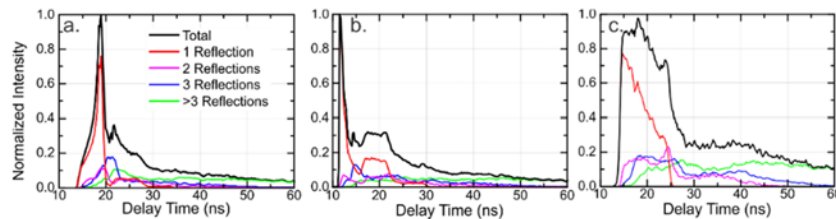


Fig. 5. Contribution of reflected light components to the Impulse Response Functions for 4-sided illumination with electrical signal input from center of the room (a) corner (15,10,0), and (b) edge (15,240,0), and (c) center (240,245,0)

Additional insight into the rms delay spread and ways to reduce it can be obtained by analyzing the impulse response function (IRF) and the contributions to the signal of the various reflection paths. Figure 5 presents the impulse response function for detectors placed at three representative points (corner, edge and center) for 4-sided illumination with the electrical signal fed into the center of each LED strip. The shape of the IRF strongly depends on the location in the room. In the corner Fig. 5(a) and side of the room Fig. 5(b), the IRF is dominated by a sharp (FWHM ~ 3 ns) peak. At the side, this sharp peak is followed by ~ 10 ns long plateau and then a gradual decay. However; in the center of the room Fig. 5(c), where the rms delay time is a maximum, the IRF function is dominated by a 10 ns wide high plateau followed by lower 15 ns wide plateau and a long tail. The initial wide plateau is dominated by photons trajectories incorporating 1, 2 or 3 reflections and the secondary plateau has equal

contributions of 2, 3, and 4 or more reflections. Finally the tail is dominated by photons undergoing 4 or more reflections.

4. Discussion and conclusions

4.1 Dependence on room reflectivity

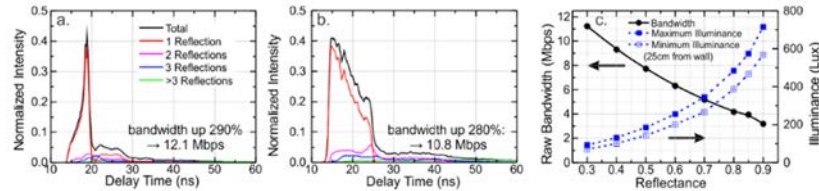


Fig. 6. Effects of decreasing reflectivity by 50% on the impulse response function for 4-sided illumination with signal input from the center. (a) edge, (b) location of maximum rms delay spread (center of room), (c) Summary of the effect of reflectivity on bandwidth and illuminance. Minimum illuminance is taken at a point 25cm from the wall. The limiting bandwidth is determined by the point in the room in which the rms delay spread is greatest.

We will focus on the location at which the maximum rms delay spread occurs as this will limit the data rate for the whole room. For 4-sided symmetrical excitation, this is the center of the room. In the previous section, we used a wall and ceiling reflectivity of $R = 0.85$, corresponding to high-quality white paint [17]. In a real office environment, it is expected that the actual wall reflectivity will be lower and thus the contribution from multiple reflections to the IRF will be considerably reduced. In [17] the reflectivity of light-colored walls is given as between $R = 0.4$ and $R = 0.6$. Figure 6 the effect of this reduced reflectivity on the IRF and the rms delay spread is presented. In Fig. 6(a) [6(b)] the IRF is presented at the edge [center] of the room (corresponding to the point in Fig. 5(b) [5(c)]) Comparing Fig. 6(a) [6(b)] with Fig. 5(b) [5(c)], the drop in reflectivity results in a 60% drop in the peak intensity, and 80% drop in illuminance at a given point (area under the IRF). At the higher reflectivity (Fig. 5) 40% of the photons experience more than 3 bounces before being detected, contributing to a long tail on the IRF while at the lower reflectivity 94% of the detected photons experience 3 or less bounces. The elimination of these higher order reflections reduces the IRF's tail resulting in a 65% drop in the rms delay spread corresponding to an over 300% increase in bandwidth to over 10Mbps. Generalizing from these two points, although the shape of the IRF varies greatly across the room, its dependence on reflectivity is similar at all points. Figure 6(c) summarizes the effect of wall reflectivity on the maximum data speed (limited by the position the room with maximum delay spread) and the room illumination. As the reflectivity of the room drops, the raw bandwidth increases and the illuminance decreases assuming that the input Lumens is held constant. (In a real lighting situation, this is unlikely to be the case – one would expect that the input number of Lumens would be increased in those rooms with darker walls in order to maintain a constant value of illuminance.)

4.2 Applications

While VLC using LED strip lighting with organic coating is not able to match the speeds obtained by direct line-of-sight systems or existing WiFi systems, its low cost and ease of implementation should allow application in systems in which speed is not crucial but availability is, e.g. Internet of Things (IoT). The system also has the potential of not only transferring information but also power in the case of low power equipment.

Compared to higher speed optical systems in which a blue filter is required [4], organic phosphors allow the use of the complete optical spectrum – a gain in irradiance of a factor of ~6. This gain in usable power is further enhanced by the fact that most available detectors peak around 760nm) with responsivity in the blue spectral region (~450nm) typically being ~20% that of the red. Combining these two factors suggests that this system can operate with

~30x lower light modulation levels and obtain the same signal to noise ratio as a system incorporating a blue filter.

A further issue that is often overlooked in optical systems is the cost of photodiodes capable of supporting speeds of 200 Mbps. For the transmission speeds at which the LED strips would operate, a photodiode response time of 5ns is sufficient, allowing the use of cheaper off-the-shelf photodiodes. Finally, it is likely equalization and advanced coding techniques, such as suggested in Ref [9], can increase significantly the bitrate.

4.3 Summary

The application of LED strip lighting with organic color converter and a single power transformer for diffuse indirect lighting and visible light communication has been investigated using Monte Carlo ray tracing simulation. Along with providing a pleasing work environment, raw data transfer rates of 10 Mbps are obtainable in a standard 5m by 5m by 3m room. We believe that such a system will find application in environments where low-cost high efficiency lighting is required and moderate download speeds are sufficient.

Funding

Ministry of Science and Technology, Taiwan (104-2112-M-155-001).